# Permafrost response and feedback under temperature stabilization and overshoot scenarios with different global warming levels

Min Cui<sup>1</sup>, Duoying Ji<sup>1</sup> and Yangxin Chen<sup>1</sup>

<sup>+</sup>Faculty State Key Laboratory of Earth Surface Processes and Disaster Risk Reduction, Faculty of Geographical Science, Beijing Normal University, Beijing, 100875, China

Correspondence to: Duoying Ji (duoyingji@bnu.edu.cn)

#### Abstract.

5

15

20

25

Permafrost regions in the northern high latitudes face faces significant degradation risks under global warming and threater the achievement of global climate goals. This study explores the response and feedback of permafrost and the associated carbon loss under temperature stabilization scenarios, where the global mean temperature stabilizes at various global warming levels, and overshoot scenarios, where the global mean temperature temporarily exceeds the 1.5 °C warming target-before returning. Under the 1.5 °C and 2 °C stabilization scenarios, permafrost area is projected to decrease by 4.6 [4.5 to 4.7] million km<sup>2</sup> and 6.6 [6.4 to 6.8] million km<sup>2</sup>, respectively, from a pre-industrial level of 17.0 million km<sup>2</sup>. Corresponding permafrost carbon losses are estimated at 54 [32 to 79] PgC and 72 [42 to 104] PgC, relative to a pre-industrial carbon stock of 484 [383 to 590] PgC. In overshoot scenarios, permafrost area shows effective recovery, with additional losses of only 0.6 [0.3 to 1.1] million km<sup>2</sup> compared to the 1.5 °C stabilization scenario. In contrast, permafrost carbon loss remains largely irreversible, with additional loss of 24 [4 to 52] PgC compared to the 1.5 °C stabilization scenario. Both stabilization and overshoot scenarios show that additional warming due to permafrost carbon feedback rises with higher global warming levels, and the most substantial feedbackadditional warming in overshoot scenarios is anticipated becomes most pronounced during the cooling phase. The additional permafrost area loss due to permafrost carbon feedback, which accounts for 5 [2 to 11] % of the total loss, is influenced by both the magnitude of additional warming and the sensitivity of permafrost area to global warming. Moreover, the responses of permafrost area, permafrost carbon, and associated radiative forcing to a broad range of global warming exhibit near-linear relationships under stabilization scenarios. PermafrostBased on the simulations presented, permafrost carbon feedback is unlikely to initiate a self-perpetuating global tipping process under both stabilization and overshoot scenarios. These findings have significant implications for long-term climate change and mitigation strategies.

## 1 Introduction

Permafrost soils in the northern high latitudes contain an estimated 1100-1700 Pg of carbon, primarily in the form of frozen organic matter, which is roughly twice the amount of carbon in the atmosphere (Hugelius et al., 2014; Schuur et al., 2015). As the climate warms, both the gradual orand abrupt permafrost thaw processes, along with subsequent microbial

decomposition, would release carbon dioxide (CO<sub>2</sub>) and methane (CH<sub>4</sub>) into the atmosphere, thereby amplifying the warming effect (Koven et al., 2011; Feng et al., 2020; Smith et al., 2022). The positive feedback mechanism, combined with the fact that warming rates in the Arctic exceed the global average (Fyfe et al., 2013; Liang et al., 2022; Rantanen et al., 2022), underscores the critical role of permafrost as a key tipping element in the climate system (Armstrong McKay et al., 2022). However, current Earth system models inadequately represent or omit the permafrost carbon processes, which has become one of the largest sources of uncertainty in future climate projections (Schädel et al., 2024). Therefore, researching the release of permafrost carbon loss and its feedback on the climate system is crucial for accurately assessing climate risks and formulating effective emission reduction strategies.

The Paris Agreement aims to limit global average temperature rise to well below 2 °C above pre-industrial levels, with efforts to keep it below 1.5 °C. Despite these goals, global warming has already exceeded 1 °C and is on track to surpass 3 °C by the end of the 21st century, primarily due to increased anthropogenic CO<sub>2</sub> emissions (Haustein et al., 2017; Hausfather and Peters, 2020). If current emission rates persist, the remaining carbon budgets compatible with the 1.5 °C target will be critically tight and likely exhausted within the next few years (Rogelj et al., 2015; Goodwin et al., 2018; Masson-Delmotte et al., 2018; Forster et al., 2023; Smith et al., 2023). It is unlikely that the 1.5 °C target set by the Paris Agreement will be met (Raftery et al., 2017). However, it might still be achievable after a period of temperature overshoot, by compensating for excessive past and near-term emissions with net-negative emissions at a later time – i.e., through on-site CO<sub>2</sub> capture at emission sources and carbon dioxide removal from the atmosphere (Gasser et al., 2015; Sanderson et al., 2016; Seneviratne et al., 2018; Drouet et al., 2021; Schwinger et al., 2022).

Several existing studies have assessed the climate response to overshoot pathways. Many components of the physical climate system have been identified as reversible, although typically with some hysteresis behavior (Boucher et al., 2012; Wu et al., 2015; Tokarska and Zickfeld, 2015; Li et al., 2020; Cao et al., 2023). In this context, reversibility refers to a partial recovery of climate conditions in an overshoot scenario toward an Earth system state without overshoot. These studies demonstrate that global mean temperature, sea surface temperature, and permafrost area can recover within decades to centuries in response to net negative emissions. Carbon releaseloss from permafrost has been shown to be irreversible on multidecadal to millennial timescales (MacDougall et al., 2013; Schwinger et al., 2022). The presence or absence of hysteresis effect in the permafrost processes is influenced by multiple factors, including the thermal inertia of permafrost soils, potential shifts in vegetation composition, and the extent to which irreversible permafrost carbon losses are offset by gains in vegetation and non-permafrostusual soil carbon reservoirs (MacDougall, 2013; Schwinger et al., 2022). Furthermore, the soil carbon loss under overshoot scenarios significantly affects the hydrological and thermal properties of soils (Zhu et al., 2019), which in turn modulate the processes involved. The interactions between physical and biophysical processes can potentially stabilize the carbon, water, and energy cycles at distinct post-overshoot equilibria (de Vrese and Brovkin, 2021). Therefore, a temporary warming of the permafrost regions entails important legacy effects and lasting impacts on its physical state and carbon cycle. However, these existing studies have yet to assess permafrost carbon feedback under overshoot scenarios.

30

40

45

55

The terrestrial component of UVic ESCM v2.10 uses the Top-down Representation of Interactive Foliage and Flora Including Dynamics (TRIFFID) vegetation model to describe the states of five plant functional types (PFT): broadleaf tree, needleleaf tree, C3 grass, C4 grass, and shrub (Cox, 2001; Meissner et al., 2003). A coupled photosynthesis-stomatal conductance model is used to calculate carbon uptake via photosynthesis, which is subsequently allocated to vegetation growth and respiration. The resulting net carbon fluxes driveprimary productivity drives changes in vegetation characteristics, including areal coverage, leaf area index, and canopy height for each PFT. The UVic ESCM v2.10 utilized in this study does not account for nutrient limitations in the terrestrial carbon cycle, leading to an overestimation of global gross primary productivity and an enhanced capacity of land to take up atmospheric carbon (De Sisto et al., 2023). However, the model reasonably represents the dominant PFTs of C3 grass, shrub, and needleleaf tree at northern high latitudes, although it underestimates vegetation carbon density over this area (Mengis et al., 2020).

100

105

110

115

120

The UVic ESCM v2.10 represents the terrestrial subsurface with 14 layers, extending to a total depth of 250.3 m to correctly capture the transient response of permafrost on centennial timescales. The top eight layers (10.0 m) are involved in the hydraulie cyclehydrologically active, while the deeper layers are modeled as impermeable bedrock (Avis et al., 2011). The carbon cycle is active in the top six layers (3.35 m), where organic carbon from litterfall, simulated by the TRIFFID vegetation model, is allocated to soil layers with temperatures above 1 °C according to an exponentially decreasing function with depth. If all soil layers are below 1 °C, the organic carbon is added to the top soil layer. The soil respiration is calculated for each layer individually as a function of temperature and moisture, but the respiration ceases when the soil layer temperature falls below 0 °C (Meissner et al., 2003; Mengis et al., 2020). In regions where permafrost exists defined as areas where soil temperature remains below 0 °C for at least two consecutive years. In permafrost regions the model applies a revised diffusion-based cryoturbation scheme to redistribute soil carbon within the soil column. Compared to the original diffusionbased cryoturbation scheme proposed by Koven et al. (2009), the revised cryoturbation scheme calculates carbon diffusion using an effective carbon concentration that incorporates the volumetric porosity of the soil layer, rather than the actual carbon concentration, thereby resolving the disequilibrium problem of the permafrost carbon pool during model spin-up (MacDougall and Knutti, 2016). However, as the UVic ESCM v2.10 only simulates permafrost carbon in the top 3.35 m of soil, the current cryoturbation scheme cannot initiate the formation of Yedoma. As a result, soil carbon stored in deep deposits of Yedoma regions is omitted in our simulations.

In the UVic ESCM v2.10, the usual soil carbon and the permafrost carbon are depicted as two distinct depth-resolved carbon pools within the upper six soil layers. Soil carbon that is transported diffused downward and crosses the permafrost table (i.e. the depth of the active layer) is transformed into permafrost carbon. Conversely, permafrost carbon that is moveddiffused upward and crosses the permafrost table is converted back into usual soil carbon. However, as the active layer deepens, thawed permafrost carbon is not transferred to the usual soil carbon pool; it remains in the permafrost carbon pool and decomposes at a rate distinct from that of usual soil carbon. Permafrost carbon can only be decomposed into CO<sub>2</sub>, as the UVic ESCM v2.10 does not include a methane production module (MacDougall and Knutti, 2016). The permafrost carbon pool is characterized by four key parameters: (1) a decay rate constant; (2) the available fraction of the pool for decomposition,

I'm confused again. This indicales 3 pools.

permatrost that has

thousand

permatrost C that has

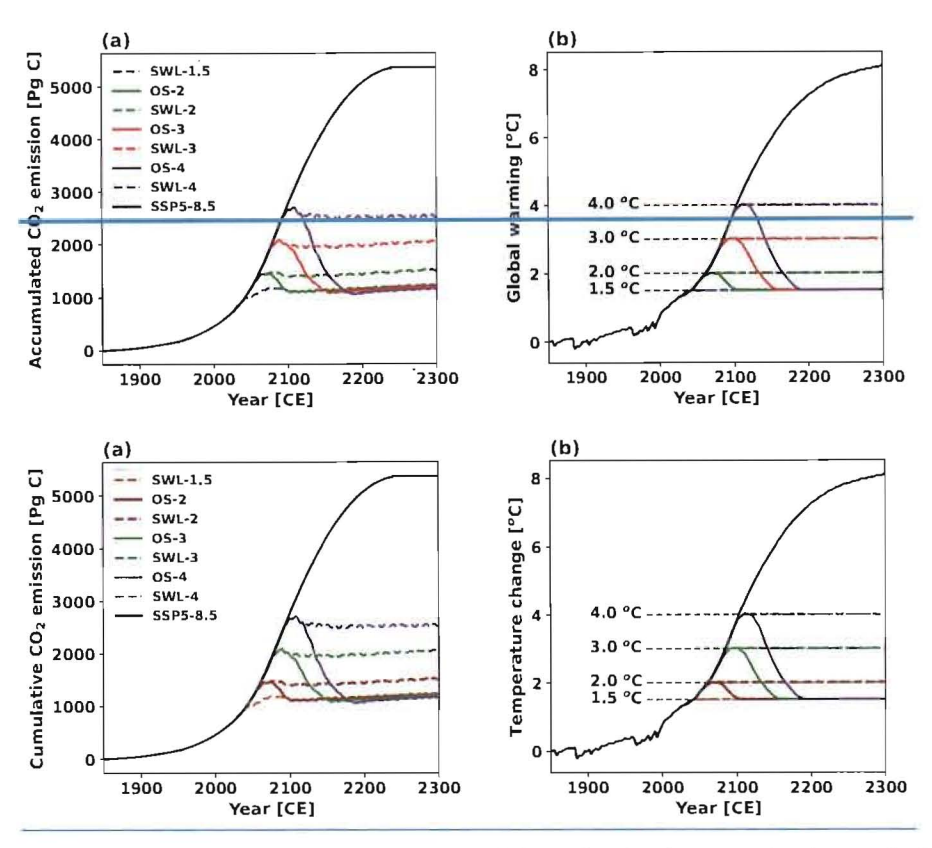


Figure 1. Temperature stabilization and overshoot scenarios designed through a simple proportional control scheme (Zickfeld et al., 2009) on CO<sub>2</sub> emission and UVic ESCM v2.10 with permafrost carbon module deactivated (corresponding to the NPFC simulations).

(a) Accumulated Cumulative CO<sub>2</sub> emission and (b) global warmingtemperature change relative to the pre-industrial levels (1850-1900), in the historical and SSP5.8.5 scenario (black), the stabilization (dashed lines) and overshoot (solid lines) scenarios at for 1.5 °C (blueorange), 2.0 °C (green linna), 3.0 °C (red)green), and 4.0 °C (purple) global warming levels.

195

200

To evaluate the uncertainty in permafrost carbon response under stabilization and overshoot scenarios, we perturbed the four key permafrost carbon parameters following the methodologies of MacDougall and Knutti (2016) and MacDougall (2021). The permafrost carbon decay constant was derived from the mean residence time (MRT) of the slow soil carbon pool at 5 °C in permafrost soils and adjusted to reflect decay at 25 °C using the method proposed by Kirschbaum (2006). The probability distribution function of mean residence time was taken as a normal distribution with a mean of 7.45 years and a standard deviation of 2.67 years from Schädel et al. (2014). The available fraction of permafrost carbon for decomposition was derived from the size of the fast, slow, and passive soil organic carbon pools separately for organic, shallow mineral, and deep mineral soils measured by Schädel et al. (2014). The probability distribution function of available fraction of permafrost carbon for decomposition was described by weighted gamma distributions, with each distribution respectively describing the probability distribution function of available fraction of permafrost carbon for decomposition in organic, shallow mineral, and deep mineral soils. The passive carbon pool transformation rate was estimated from the <sup>14</sup>C age of the passive carbon pool from midlatitude soils (Trumbore, 2000). Its mean residence time at 5 °C is 300 to 5000 years, yielding an estimated value

Not defined yet

passive carbon pool transformation rate of 0.25×10<sup>-10</sup> to 4×10<sup>-10</sup> s<sup>-1</sup> (Trumbore, 2000). after adjustment to 25 °C. The probability distribution function mean residence time of the passive carbon pool transformation rate was taken as assumed to follow a uniform in base two logarithmic spacedistribution (MacDougall and Knutti, 2016). For the initial quantity of total permafrost region soil carbon, its probability distribution function was taken as a normal distribution with a mean of 1035 PgC and a standard deviation of 75 PgC, informed by Hugelius et al. (2014). A series of 5,000-year sensitivity runs were performed under preindustrial steady conditions with varying saturation factors to determine their relationship with the quantity of the total permafrost region soil carbon bool. This relationship was then utilized to tune the total permafrost region soil carbon pool, ensuring alignment with observational data (Hugelius et al., 2014). Fig. 2 illustrates the probability distribution function for each perturbed parameter. MacDougall and Knutti (2016) and MacDougall (2021) additionally perturbed two physical climate parameters controlling climate sensitivity and Arctic amplification, but they are not perturbed in this study due to their limited influence on global mean temperature in stabilization scenarios.

The Latin hypercube sampling method (McKay et al., 1979) was used to explore the effects of parameter uncertainty on projections of permafrost carbon change. In this study, the probability distribution function of each key permafrost carbon parameter was divided into 25 intervals of equal probability. One value was randomly selected from each interval for a given parameter, and then randomly matched with values of the other three key parameters selected in the same manner to generate parameter sets. This sampling procedure was repeated 10 times, resulting in 250 unique parameter sets (i.e., 250 model variants). For each parameter set, the UVic ESCM v2.10 was first run through a 10,000-year spin-up phase under pre-industrial conditions to achieve a quasi-equilibrium state. For these spin-up runs, the atmospheric CO<sub>2</sub> concentration was fixed at 284.7 ppm and the solar constant was set to 1360.747 W m<sup>-2</sup>. Following the spin-up, emission-driven transient simulations were conducted under the stabilization, overshoot, and SSP5-8.5 scenarios. The results are presented as the median across all model variants, with uncertainty quantified as the range between the 5th to the 95th percentiles.

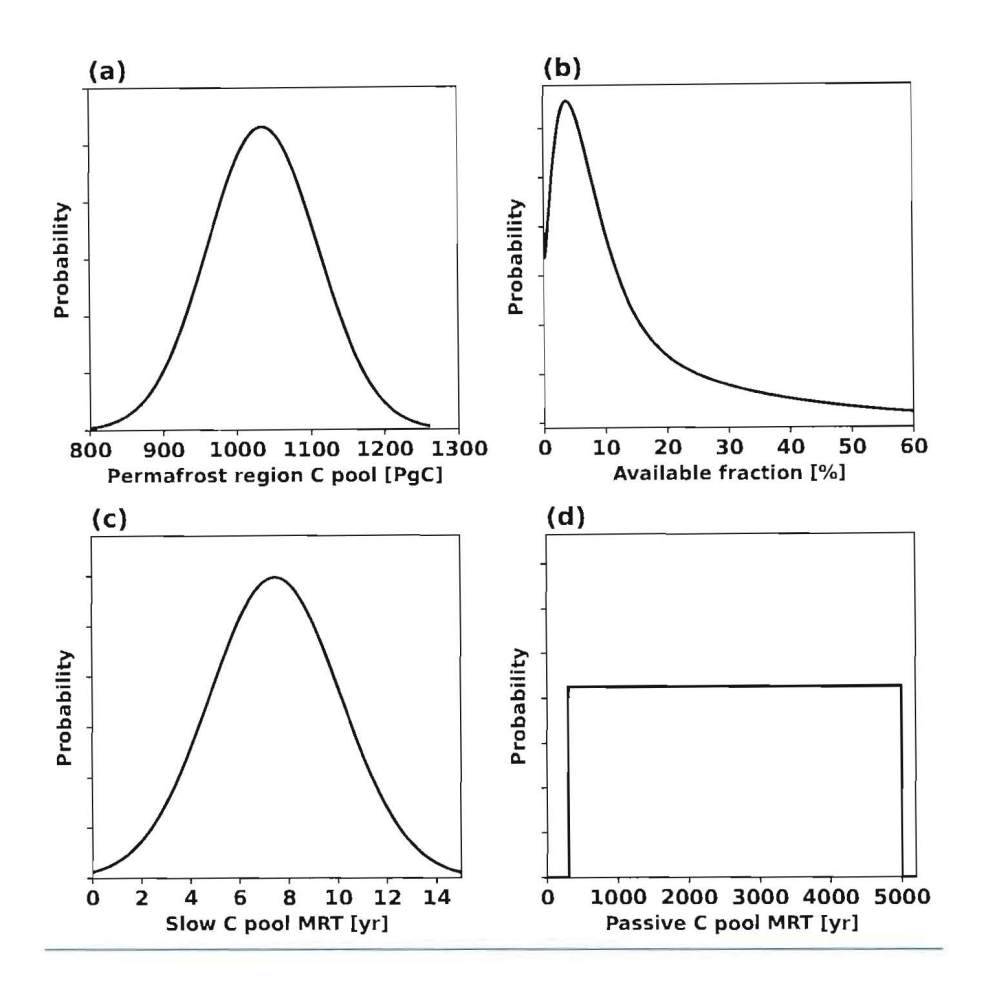


Figure 2. Probability distribution functions of the four key permafrost carbon parameters perturbed in the UVic ESCM v2.10 to represent uncertainty in permafrost carbon response. Panel (d) employs a logarithmic scale on the horizontal axis to better illustrate the distribution of the corresponding parameter. This figure is reproduced This figure is adapted from MacDougall (2021).

#### 3 Results

235

240

The UVic ESCM v2.10 reliably simulates historical temperature changes, permafrost area, and the partitioning of anthropogenic permafrost carbon-emissions among the atmosphere, ocean and land, and total permafrost region soil carbon stocks. Under pre-industrial conditions, the simulated Northern Hemisphere permafrost area, defined as regions where the soil layer remains perennially frozen for at least two consecutive years, was 17.01 [17.00 to 17.04] million km², the simulated total soil carbon stock in the permafrost regions was 1031 [915 to 1149] PgC, of which 484 [383 to 590] PgC was classified as perennially frozen permafrost carbon and 547 [533 to 559] PgC was classified as usual soil carbon. For the period 1960–1990, the model simulated Northern Hemisphere permafrost area at 16.8 [16.7 to 16.9] million km², which falls within the reconstructed range from 12.0 to 18.2 million km² (Chadburn et al., 2017) and the observation derived extent from 12.21 to

"total perma forst region soil carbon" on page 8.

16.98 million km² (Zhang et al., 2000). Additionally, the simulated total soil carbon stock in the top 3.35 m of permafrost regions for this same period was 1034 [919 to 1151] PgC, with 483 [382 to 587] PgC classified as perennially frozen permafrost carbon, accounting for 47% [42% to 51%] of the total permafrost region soil carbon stock, in agreement with Hugelius et al. (2014). Note that the permafrost area is defined as the area where soil temperature remains below 0 °C for at least two consecutive years, whereas for carbon-related variables the permafrost region is defined as the area where permafrost carbon exceeds zero in UVic ESCM. The area with non-zero permafrost carbon is 17.2 million km² and changes only minimally throughout the simulations.

The UVic ESCM v2.10 also realistically simulates historical temperature changes and the partitioning of anthropogenic carbon emissions among the atmosphere, ocean and land. During the period 2011–2020, the model estimated a global mean temperature increase of 1.14 [1.13 to 1.15] °C relative to preindustrial levels, which is closely aligned with the observed rise of 1.09 [0.91 to 1.23] °C (Gulev et al., 2021). From 2010 to 2019, the model estimated that anthropogenic carbon emissions of 11 PgC yr<sup>-1</sup> were distributed as follows: 5.5 [5.4 to 5.6] PgC yr<sup>-1</sup> to the atmosphere, 3.0 [2.98 to 3.03] PgC yr<sup>-1</sup> to the ocean, and 2.5 [2.4 to 2.6] PgC yr<sup>-1</sup> to terrestrial ecosystems. These estimates are broadly consistent with the global anthropogenic CO<sub>2</sub> budget assessment by the Global Carbon Project (GCP) with figures of 5.1±0.02 PgC yr<sup>-1</sup> for the atmosphere, 2.5±0.6 PgC yr<sup>-1</sup> for the ocean, and 3.4±0.9 PgC yr<sup>-1</sup> for terrestrial ecosystems (Friedlingstein et al., 2020).

# 3.1 Permafrost Response

245

250

255

260

265

270

The Northern Hemisphere high-latitude permafrost area is strongly correlated with changes in global mean temperature (Fig. 3a, b; Fig. S1a, b). As global warming increases from 1.5 °C to 4 °C, the permafrost area declines from 13.9 to 8.3 million km<sup>2</sup> under the SSP5-8.5 scenario, by year 2300. In the stabilization scenarios, when global warming is stabilized at the Paris Agreement targets of 1.5 °C or 2 °C, permafrost degradation is effectively suppressed compared to the SSP5-8.5 scenario. By 2300, permafrost area decreases by 4.6 [4.5 to 4.7] million km<sup>2</sup> and 6.6 [6.4 to 6.8] million km<sup>2</sup> from the pre-industrial level of 17.0 million km<sup>2</sup> under SWL-1.5 and SWL-2 scenarios, respectively, accounting for 39 [38 to 40] % and 56 [54 to 58] % of the reduction observed under SSP5-8.5 scenario. The incremental additional permafrost degradation under the SWL-3 compared to SWL-2 is significantly larger than that under SWL-4 compared to SWL-3. This is mainly because the remaining permafrost available for degradation becomes progressively limited under higher global warming levels, and the permafrost area under higher stabilization scenarios has not yet reached a steady state in our simulations. Additionally, the permafrost area under the SWL-3 and SWL-4 scenarios exceeds that under the SSP5-8.5 scenario by only 2.0 [1.9 to 2.1] million km<sup>2</sup> and 0.9 [0.8 to 1.0] million km<sup>2</sup> by 2300, respectively. This is primarily because the permafrost area in the SSP5-8.5 scenario is smaller and, as a transient simulation, is further from equilibrium compared to SWL-3 and SWL-4. However, during the cooling phase of the overshoot scenarios, as the global mean temperature returns to 1.5 °C above pre-industrial levels, the permafrost area gradually recovers to that under the SWL-1.5 scenario (Fig. 4a; Fig. S2a). By 2300, it converges to similar levels of 11.1~12.4 million km<sup>2</sup> under the OS-2, OS-3 and OS-4 scenarios, with an additional loss of only 0.2~1.2 million km<sup>2</sup> compared to the SWL-1.5 scenario. This indicates that permafrost area is nearly reversible and largely follows the global mean

to the top soil layer. Meanwhile, permafrost carbon and non-permafrost susual soil carbon are both represented as depth-resolved carbon pools within the top six soil layers. The movement of permafrost carbon due to cryoturbation mixing is parameterized as being proportional to the gradient of total soil carbon with depth. Soil carbon that diffuses downward through the permafrost table is converted to permafrost carbon. During the cooling phase of overshoot scenarios, increased litterfall and a rising permafrost table lead to elevated carbon concentrations in surface soil layers, resulting in enhanced vertical diffusion and a surge in permafrost carbon inputs. Conversely, under the SSP5-8.5 scenario, permafrost carbon inputs exhibit only a minor peak around the 2150s, followed by a sharp decline (Fig. 5a; Fig. S3a). This is due to the continuous reduction in permafrost area and the deepening of the permafrost table, both of which reduce carbon concentrations in the upper soil layers and weaken vertical diffusion, despite the increasing litter flux under a strong CO<sub>2</sub> fertilization background. We note that the approach adopted in the model may not accurately describe natural processes of vertical carbon movement, which are influenced by soil porosity heterogeneity, freeze-thaw cycles, and ice expansion upon freezing.

325

335

340

350

355

Permafrost Total permafrost region soil carbon shows a strong tendency to recover after temperature overshoot-(Fig. 3d). In contrast, total permafrost region soil carbon continues to decrease under temperature stabilization scenarios, but the rate of decrease is gradually slowing down. The total permafrost region soil carbon releaseloss in the overshoot scenarios is significantly mitigated compared to stabilization scenarios at same global warming levels (Fig. 3d; Fig. S1d). By 2300, total permafrost region soil carbon losses under OS-2, OS-3, and OS-4 scenarios are projected to be 41 [15 to 72], 61 [29 to 98], and 81 [44 to 124] PgC, respectively, with reductions of 14 [8 to 21], 41 [25 to 57], and 62 [41 to 82] PgC compared to the SWL-2, SWL-3, and SWL-4 scenarios, respectively. During the stabilization phase in the overshoot scenarios, additional total permafrost region soil carbon losses compared to the SWL-1.5 scenario continue to decrease, but the total permafrost region soil carbon in the overshoot scenarios does not fully recover to the level under the SWL-1.5 scenario by 2300 (Fig. 4c; Fig. S2c). Notably, in all stabilization and overshoot scenarios simulated in this study, the permafrost region soil serves as a net cumulative carbon source for atmospheric CO<sub>2</sub> by 2300. However, during the stabilization phase of OS-3 and OS-4, the permafrost region soil turns into a carbon sink, as soil carbon inputs surpass the reduced decomposition activity due to the depletion of soil carbon stocks and reduced warming levels. Permafrost Total permafrost region soil carbon inputs primarily originate from-robust biophysical processes related to vegetation litterfall, with their intensity influenced by warming levels and CO<sub>2</sub> fertilization effects, while total permafrost region soil carbon decomposition is closely tied to global mean temperature. In the overshoot scenarios, the peak for total permafrost region soil carbon inputs occurs slightly later than the global mean temperature peak, whereas the peak for total permafrost region soil carbon decomposition happens marginally earlier than the global mean temperature peak (Fig. 5b, d; Fig. S3b, d).

The total permafrost region soil carbon inputs generally track the trajectory of litter flux across the same area, with an approximate delay of 10-20 years (not shown). To attribute the contribution of total permafrost region soil carbon inputs, we examined how dominant vegetation types (needleleaf tree, C3 grass and shrub) over the permafrost region adapt to temperature and atmospheric CO<sub>2</sub> concentrations in both overshoot and stabilization scenarios (Fig. 6). Needleleaf trees expand slowly and continuously in the permafrost region in both overshoot and stabilization scenarios, whereas that of shrubs closely follows the

ishet does that's refers to?

# simulations? Why the use of "expected"?

trajectory of global mean temperature. The combined areal coverage of trees and shrubs is projected to cover about 62% upon Upon 1.5 °C warming (projected for the 2040s relative to pre-industrial levels around 2040s 1850–1900), trees and shrubs are expected to cover approximately 62% of the area where permafrost carbon is non-zero, slightly higher than the 24~52% range projected for 2050 using a statistical approach that links climate conditions to vegetation types under two distinct emission trajectories (Pearson et al., 2013). During the warming and cooling phases of overshoot scenarios, the expansion and reduction of shrubs correspond with the degradation and expansion of C3 grasses, respectively. Among the three dominant PFTs, only shrubs show a nearly reversible response in areal coverage, net primary productivity (NPP) and vegetation carbon with respect to global mean temperature under overshoot scenarios. In contrast, the continuous reduction of C3 grasses and the expansion of needleleaf trees suggest a degree of irreversibility in the structure and vegetation carbon density of northern high latitude terrestrial ecosystems under overshoot scenarios. Our results are in line with an earlier study by Tokarska and Zickfeld (2015), but contrast with Schwinger et al. (2022) who reported only minor differences in vegetation carbon after the overshoots compared to the reference simulation with no overshoot by prescribing vegetation distributions. In our study, the shifts in vegetation composition and changes in living biomass, especially those associated with woody vegetation, are key drivers of total permafrost region soil carbon inputs.

The uncertainty in total permafrost region soil carbon releaseloss is nearly the same as that of permafrost carbon releaseloss (Fig. 3c, d; Fig. S1c, d). For example, the 5th to 95th percentile range of total permafrost region soil carbon releaseloss under the OS-2 and OS-4 scenarios is 58 PgC and 81 PgC respectively by 2300, compared to 52 PgC and 72 PgC for permafrost carbon releaseloss. This indicates that the uncertainty in total permafrost region soil carbon releaseloss is largely driven by the uncertainty in permafrost carbon releaseloss. Therefore, we evaluate the relative importance of perturbed permafrost carbon parameters on total permafrost region soil carbon releaseloss under different temperature pathways through calculating their correlations across all ensemble simulations. The influence of model parameters on the uncertainty of permafrost carbon losses by 2300 is relatively consistent across the SSP5-8.5, OS-4, and SWL-4 scenarios, with the strongest correlations observed for the permafrost passive carbon pool transformation rate (R=0.81~0.85), followed by the initial quantity of total permafrost region soil carbon (R=0.55~0.61). This finding aligns with Ji et al. (2024), who highlights the critical role of these two parameters in the uncertainty of total permafrost region soil carbon loss under temperature overshoot and 1.5 °C warming stabilization scenarios.

to result in enough additional thawing and corresponding carbon emissions to initiate a self-perpetuating tipping process. Since this study only models the gradual thawing of permafrost through the deepening of the active layer, we cannot rule out the possibility of tipping points associated with the abrupt thawing of talik development, thermokarst and thermo-erosion processes.

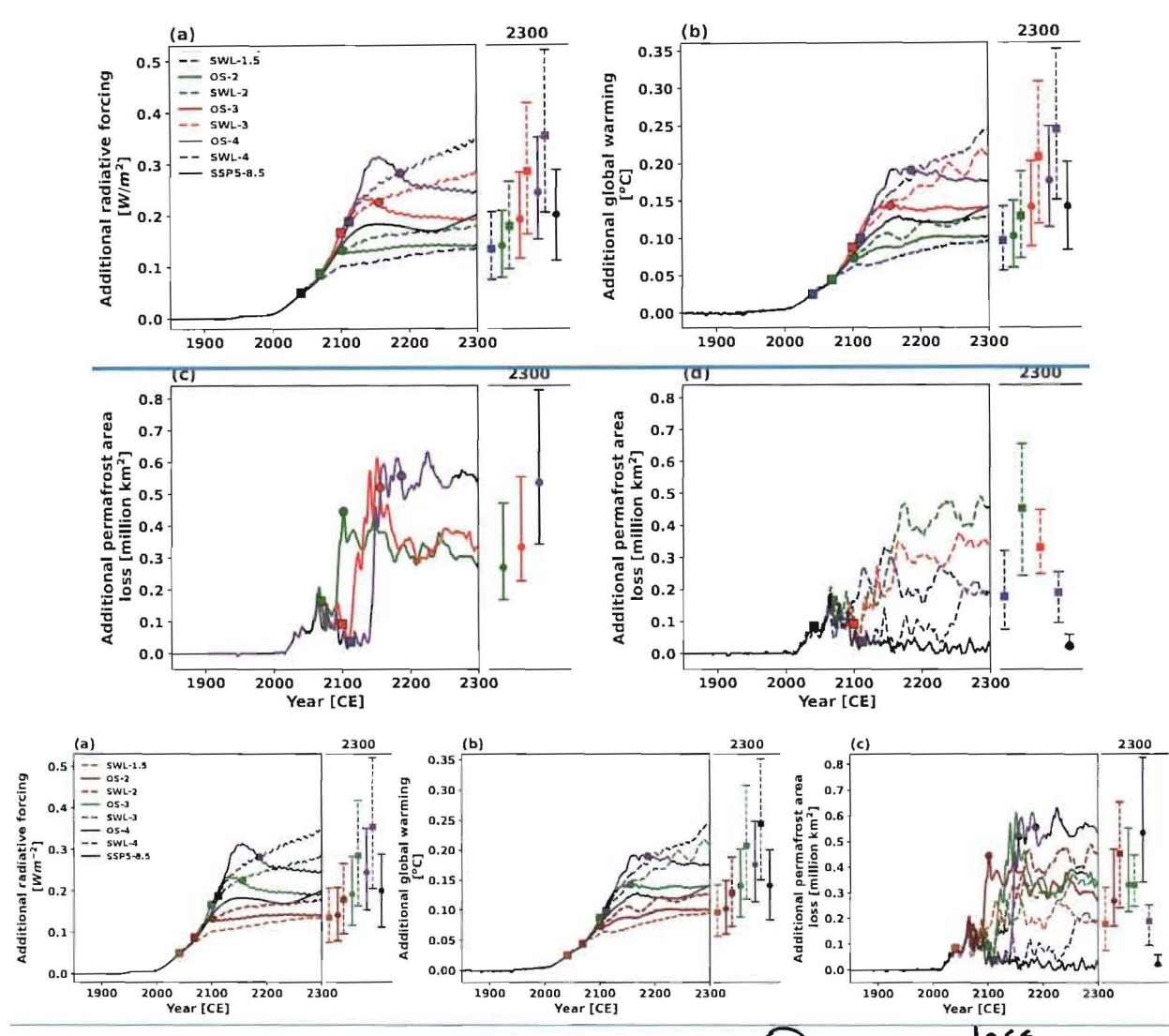


Figure 7. Additional stress in (a) radiative forcing, (b) global warming and (c, d) termafrost area due to permafrost carbon feedback, calculated as the difference between the PFC and NPFC simulations. ShownResults are results for the shown under stabilization (dashed lines) and overshoot (solid lines) scenarios at for 1.5 °C (blue orange) 2.0 °C (green sienna), 3.0 °C (red) green), and 4.0 °C (purple) global warming levels, along with the SSP5-8.5 scenario (black). Square markers indicate the time points when the temperature overshoot reaches its peak or stabilized warming begins, while circle markers indicate when the overshoot returns to 1.5 °C. Results represent the ensemble median of 250 simulations. Dots on the adjacent right panels represent values in the year 2300, with uncertainty ranges estimated as the 5th to 95th percentiles. In panel (a), the additional radiative forcing is calculated

455

460

we don't have panel d'any more

21

loss and associated radiative forcing exhibit a nearly linear response to increasing global warming levels, especially above l °C, for both stabilization and SSP5-8.5 scenarios (Fig. 10b, c).

520

525

530

535

540

545

550

Meanwhile, the sensitivities of permafrost area, permafrost carbon loss, and associated radiative forcing to global warming under stabilization scenarios are all stronger than those under the SSP5-8.5 scenario. Specifically, based on the simulated permafrost area in the year 2300 under stabilization scenarios with global warming levels between 1.5 °C and 3 °C, the sensitivity of permafrost area to global warming is -3.19 [-3.01 to -3.36] million km<sup>2</sup> °C<sup>-1</sup>. In comparison, a linear fit of permafrost area change against global warming levels over the same temperature range in the SSP5-8.5 scenario yields a sensitivity of -2.85 [-2.77 to -2.89] million km<sup>2</sup> °C<sup>-1</sup>. Similarly, the permafrost carbon feedback per degree of global warming derived from a linear fit based on the total permafrost carbon loss in the year 2300 under stabilization scenarios, is -27.6 [-16.5 to -38.2] PgC °C-1. In contrast, the corresponding value under the SSP5-8.5 scenario, estimated from a linear fit over the 1.5 °C to 4.0 °C warming range, is -19.3 [-15.7 to -24.1] PgC °C<sup>-1</sup>. Applying the same approach, the associated radiative forcing per degree of global warming is estimated to be 0.08 [0.05 to 0.12] W m<sup>-2</sup> °C<sup>-1</sup> for the stabilization scenarios and 0.04 [0.03 to 0.05] W m<sup>-2</sup> °C<sup>-1</sup> for the SSP5-8.5. These differences between the stabilization and SSP5-8.5 scenarios are mainly attributable to the differing response time scales represented by the two scenarios: SSP5-8.5 reflects a typical transient response, while the stabilization scenarios maintain stabilized temperatures over extended periods and thus approximate a quasi-equilibrium response of the climate-carbon system. Furthermore, the smaller sensitivity of permafrost radiative forcing per degree of global warming under the SSP5-8.5 can be partially attributed to its higher background atmospheric CO2 concentration compared to the stabilization scenarios. The same amount of CO<sub>2</sub> emissions would produce smaller additional radiative forcing under a higher background atmospheric CO2 concentration, due to the logarithmic relationship between CO2 concentration and radiative forcing (Etminan et al., 2016).

To a certain extent, our findings align with those of Nitzbon et al. (2024), who suggested that the accumulated response of Arctic permafrost to climate warming is approximately quasilinear. Nitzbon et al. (2024) reported a quasilinear decrease in the equilibrium permafrost extent to global warming, with a rate of approximately 3.5 million km² °C⁻¹. This quasilinear relation holds for global warming ranges from 0 °C to 4 °C, derived from the empirical relationship between the local permafrost fraction and the annual mean global temperature. However, our results indicate the quasilinear relationship only holds for global warming levels between 1.5 °C and 3 °C. Furthermore, the permafrost carbon feedback and the associated radiative forcing per degree of warming, as derived from our simulations of both stabilization and SSP5-8.5 scenarios, are within the ranges of -18 [-3.1 to -41] PgC °C⁻¹ and 0.09 [0.02 to 0.20] W m⁻² °C⁻¹, respectively, reported by Canadell et al. (2021). Our estimates also align with the estimated range of equilibrium sensitivity of permafrost carbon decline to global warming, which is -21 [-4 to -48] PgC °C⁻¹ (Nitzbon et al., 2024). This may represent an upper limit for bound on the permafrost carbon feedback per degree of global warming—considering that the estimated reduction in permafrost: the estimate reflects the maximum carbon does not equate directly tothat could be lost from frozen soils, yet only a fraction of that carbon emissions is ultimately released into the atmosphere, as noted by Nitzbon et al. (2024).

26

C lost from frozen & rils # C entering the atmosphere why?

## 4 Conclusions and Discussion

575

580

585

590

595

600

This study utilizes the intermediate-complexity Earth system model UVic ESCM v2.10 and perturbed parameter ensemble modelling approach to study the response and feedback of permafrost under temperature stabilization and overshoot scenarios across different global warming levels. The UVic ESCM v2.10 has been validated against observational and reconstructed datasets, demonstrating its ability to reproduce historical observation-based permafrost area and permafrost carbon stocks: for the present day. In addition to presenting the changes in permafrost area, permafrost carbon, and total permafrost region soil carbon under various warming trajectories, this study also quantifies the additional radiative forcing, global warming, and permafrost area loss induced by permafrost carbon releaseloss and suggests that permafrost carbon feedback is unlikely to initiate a self-perpetuating global tipping process under both stabilization and overshoot scenarios. In addition, this study reveals quasilinear responses of permafrost area, permafrost carbon, and associated radiative forcing toover a broad range of global warmingtemperature change, providing insights into the implications of permafrost carbon feedback for long-term climate change and mitigation strategies.

Reductions in permafrost area and carbon exhibit a strong correlation with global warming underfor both stabilization and overshoot scenarios. In stabilization scenarios, lower global warming levels effectively mitigate permafrost degradation compared to the SSP5-8.5 scenario, whereas higher global warming levels lead to substantial permafrost degradation due to cumulative warming effects. In overshoot scenarios, permafrost area largely recovers as global warming returns to 1.5 °C levels, though this recovery is delayed by hysteresis effects, with degradation persisting for decades after temperature peaks. Permafrost carbon declines under both stabilization and overshoot scenarios, driven by the dynamic balance between soil carbon inputs and decomposition. The overshoot scenarios partially mitigate permafrost carbon losses compared to the stabilization scenarios at the same global warming levels. Significant carbon losses persist during the cooling and stabilization phases of overshoot scenarios, highlighting the essentially irreversible nature of this process. PermafrostTotal permafrost region soil carbon exhibits a certain degree of recovery under the overshoot scenarios. In fact, soil in these regions even transitions into a carbon sink during the stabilization phase of the overshoot scenarios with high global warming levels, supported by reduced decomposition rates and sustained inputs from vegetation litterfall. However, the higher the overshoot levels, the less recovery there is. These findings underscore the critical role of temporary temperature overshooting levels in affecting long-term permafrost carbon releaseloss and recovery potential.

The responses of permafrost area, permafrost carbon, and associated radiative forcing to a broad range of global warming are nearly linear. The permafrost area and global mean temperature exhibit a quasilinear relation for the global warming ranges from 1.5 °C to 3 °C in both the stabilization and SSP5-8.5 scenarios. The permafrost carbon loss and associated radiative forcing exhibit a quasilinear relation to global warming ranges from 1 °C to 4 °C under the stabilization and SSP5-8.5 scenarios. The sensitivity of permafrost area to global warming derived from the stabilization and SSP5-8.5 scenarios is much substantially higher than 1.6 million km<sup>2</sup> °C<sup>-1</sup> derived through an equilibrium permafrost model (Liuthe estimates obtained using the Stefan solution (Peng et al., 2021-2023), but our result is close to that derived from an observation-

I think, it's ok to mention the lower number of 1.6 MICm²/·c

Should Mis J'm looking aa.

605

610

615

625

630

635

(see Figure 9a)

constrained equilibrium projection, approximately 3.5 million km² °C-¹ (Nitzbon et al., 2024). Nitzbon et al. (2024) noted that permafrost area decreases quasi-linearly with increasing global mean temperature. However, we found that the relationship holds most strongly for the global warming ranges from 1.5 °C to 3 °C. According to the SSP5-8.5 simulations, the sensitivity of permafrost area to global warming reaches its peak below 1.5 °C global warming. It then decreases to a relatively stable level between 1.5 °C and 3 °C varming levels, and continues to decline beyond the 3 °C varming level. This is in line with Comyn-Platt et al. (2018), who found the feedback processes due to permafrost thaw respond more quickly at temperatures below 1.5 °C. The maximal sensitivity occurring just below 1.5 °C global warming level suggests the fastest permafrost degradation is anticipated to take place within Paris Agreement's warming levels. Our findings have significant implications for the development of mitigation and adaptation strategies addressing permafrost-thaw impacts consistent with keeping global warming at the Paris Agreement's levels.

Our study highlights the substantial permafrost carbon feedback during the cooling phase of overshoot scenarios. Permafrost carbon releaseloss evidently increases global radiative forcing and amplifies global warming. The permafrost carbon feedback can be more profound in temperature stabilization and overshoot scenarios than in high-emissions scenarios. In stabilization scenarios, additional radiative forcing and warming persistently increase over time due to delayed degradation and from permafrost carbon loss continue to rise after temperature stabilizes, driven by delayed permafrost thaw and the attendant positive permafrost carbon feedback. In overshoot scenarios, additional warming almost stabilizes once global warming drops to 1.5 °C levels. During the cooling phase of overshoot scenarios, lower background CO<sub>2</sub> concentrations amplify the warming effect of permafrost carbon releaseloss. In contrast, under the high-emissions SSP5-8.5 scenario, the additional warming is limited due to higher background CO<sub>2</sub> levels reducing the additional radiative forcing from permafrost carbon releaseloss. The additional permafrost area loss due to permafrost carbon feedback occupies around 5 [2 to 11] % of the total loss by 2300 in the stabilization and overshoot scenarios. These This additional permafrost area losses can be well explained by the sensitivity of permafrost area to global warming and the magnitude of additional warming. The complex interactions between global warming and permafrost degradation emphasize the importance of accounting for these nonlinear effects in climate projections, particularly at 1.5~2 °C global warming levels.

Our results show incomplete recovery of permafrost area under the overshoot scenarios, which is influenced by multiple factors: First, the additional permafrost carbon releaseloss leads to greater additional warming under the overshoot scenarios than the SWL-1.5 scenario, causing additional permafrost degradation. By 2300, the northern high-latitude permafrost regions are 0.01~0.13 °C warmer compared to the SWL-1.5 scenario. Second, the thermal inertia of deep soil layers limits the rate of permafrost recovery. Even after global mean temperatures return to the 1.5 °C target, residual heat accumulated in deeper soil layers during temperature overshoot period continues to inhibit permafrost refreezing, preventing full restoration to its preovershoot state. Third, greater soil carbon loss under overshoot scenarios substantially than in the SWL-1.5 scenario alters the hydrological and thermal properties of soil, affecting the processes that govern carbon cycling (Zhu et al., 2019; Avis, 2012; Lawrence and Slate, 2008), which in turn affects the recovery of permafrost area. Moreover, irreversible shifts in vegetation composition of high-latitude terrestrial ecosystems also contribute to the incomplete recovery of permafrost area under

overshoot scenarios. For instance, among the two dominant vegetation types, needleleaf trees continue to expand while C3 grasses decline, even after global temperatures return to the 1.5 °C warming level. These irreversible changes may stabilize the carbon, water, and energy cycles over the permafrost region at different equilibria after overshoot, through the interactions between physical and biophysical processes (de Vrese and Brovkin, 2021), thereby constraining the ability of permafrost to fully recover under the overshoot scenarios.

640

645

650

655

660

665

Although permafrost carbon loss is essentially irreversible, overshoot scenarios exhibit a certain degree of recovery relative to the SWL-1.5 stabilization scenario (Fig. 4b; Fig. S2b). It is therefore eurious cientifically interesting to know whether permafrost carbon under overshoot scenarios will eventually converge with that under SWL-1.5. Our results show that permafrost carbon inputs are consistently higher under overshoot scenarios than under SWL-1.5, while permafrost carbon decomposition differ only slightly between the two (Fig. 5a, c; Fig. S3a, c). This tends to suggest that the smaller permafrost carbon stocks under overshoot scenarios by 2300 would eventually catch up to the levels under SWL-1.5. To assess this potential convergence, we extended our simulations of both SWL-1.5 and overshoot scenarios to the year 2400 (data not shown). Then we estimated the convergence time by calculating the ratio between the difference in permafrost carbon stocks and the difference in net permafrost carbon inputs (i.e., annual permafrost carbon inputs minus decomposition) for the overshoot scenarios relative to the SWL-1.5 scenario. Based on simulation results for the year 2300, the median estimated convergence times for OS-2, OS-3 and OS-4 are 1076, 1008 and 1433 years, respectively. When using results from the year 2400, the corresponding estimates increase to 1377, 1199 and 1568 years. This means that convergence would take even longer if estimated from later simulation results, mainly due to gradually weakened permafrost carbon inputs. The relatively larger permafrost carbon inputs under overshoot scenarios result mainly from increased litterfall during the overshoot phase. The extra litterfall during the overshoot phase gradually moves through the active layer and is transported to the permafrost zone. Over time, however, the effect of this extra litterfall gradually diminishes, leading to a reduction in permafrost carbon inputs. Consequently, it may take extremely long timescales for the overshoot scenarios to fully converge with SWL-1.5 in terms of permafrost carbon stocks. In addition, due to incomplete recovery of permafrost area and persistent changes in surface climate and soil properties, the overshoot scenarios might ultimately fail to converge to SWL-1.5 scenario in terms of permafrost carbon stocks.

Different permafrost carbon releaseloss and associated additional warming under overshoot scenarios confirm the path-dependent fate of permafrost region soil carbon (Kleinen and Brovkin, 2018) and the path-dependent reductions in CO<sub>2</sub> emission budgets (MacDougall et al., 2015; Gasser et al., 2018). As Since the permafrost carbon washas accumulated very slowly during the last millions few tens of thousands of years, its releaseloss would be tacked onto the anthropogenic CO<sub>2</sub> emissions, and the resulting additional warming poses a challenge to achieving global climate goals by substantially reducing the remaining carbon budget compatible with the Paris Agreement (MacDougall et al., 2015; Natali et al., 2021). In the overshoot scenarios simulated in this study, permafrost carbon releaseloss by 2300 ranges from 60 [35 to 87] PgC to 97 [63 to 135] PgC. The associated resulting additional warming caused by from the release permafrost carbon loss ranges from 0.10 [0.06 to 0.15] °C to 0.18 [0.11 to 0.25] °C. This permafrost carbon feedback contributes a substantial addition on top of 1.5 °C

one 1. of what? burden are it of mospheric corrients?

required?

warming target under overshoot scenarios, and the magnitude of this additional warming rises with the amplitude of overshoot. To accomplish the 1.5 °C target under the OS-2, OS-3, and OS-4 scenarios, anthropogenic carbon emissions would be reduced by amounts equivalent to the permafrost carbon releaseloss. The proportion of carbon removal required to offset permafrost emissions is estimated at 4.9 [2.9 to 7.1] %, 6.5 [4.1 to 9.2] %, and 8.3 [5.4 to 11.6] % by 2300, respectively. Our findings are consistent with previous research utilizing the Monte Carlo ensemble method to evaluate the response of permafrost carbon and its influence on CO<sub>2</sub> emission budgets under overshoot scenarios targeting a 1.5 °C warming limit (Gasser et al., 2018). Specifically, for overshoot amplitudes of 0.5 °C (peak warming of 2 °C) and 1 °C (peak warming of 2.5 °C), the reductions in anthropogenic CO<sub>2</sub> emissions due to permafrost are estimated to be 130 (with a range of 30–300) Pg CO<sub>2</sub> and 210 (with a range of 50–430) Pg CO<sub>2</sub>, respectively, to meet the long-term 1.5 °C target (Gasser et al., 2018). These results are comparable to our estimates of 60 [35 to 87] PgC under OS-2 and 78 [50 to 111] PgC under OS-3. The differences between the two studies can be partly attributed to different warming trajectories to achieve the same 1.5 °C target. Our study further confirms that ifdeploying negative CO<sub>2</sub> emissions were to be used to reverse the anthropogenic elimate change, the delayedwarming would be undermined by substantial post-peak warming arising from permafrost carbon release would reduce its loss, thereby diminishing their overall effectiveness (MacDougall, 2013; Tokarska and Zickfeld, 2015).

675

680

685

690

695

700

705

This study does not simulate the changes of deep Yedoma carbon under the temperature stabilization and overshoot scenarios. Yedoma deposits represent a significant deep carbon reservoir and are widespread across Siberia, Alaska, and the Yukon region of Canada, having primarily formed during the late Pleistocene, especially in the late glacial period. These deep, perennially frozen sediments are particularly ice-rich, and the freeze-locked organic matter in such deposits can be re-mobilized on short time-scales, representing one of the most vulnerable permafrost carbon pools under future warming scenarios (Schuur et al., 2015; Strauss et al., 2017). According to Zimov et al. (2006), these perennially frozen Yedoma sediments cover more than I million km<sup>2</sup>, with an average depth of approximately 25 m. Recent estimates place the organic carbon stock in Yedoma deposits at 213 ± 24 PgC, constituting a significant portion of the total permafrost carbon stocks (Strauss et al., 2017). However, the UVic ESCM v2.10 utilized in this study simulates permafrost carbon only within the top 3.35 m of soil, limiting our ability to directly assess the impacts of temperature overshoot on deep Yedoma carbon. Considering their ice-rich nature and potential susceptibility to rapid-thaw processes, we analyzed the average and maximum active layer thickness (ALT) in Yedoma regions (Strauss et al., 2021, 2022) under the simulated scenarios to approximate potential impacts. We find that the average ALT in Yedoma regions remains below 1 m in all stabilization and overshoot scenarios, while the maximum ALT rarely exceeds 3.35 m in overshoot scenarios but does exceed this depth in some stabilization scenarios. However, in all scenarios, the maximum ALT does not exceed 6 m, which is relatively shallow compared to the average depth (~25 m) of Yedoma deposits (Figure S6). Consequently, the impact on Yedoma is considered expected to be minimal in all scenarios, and the effect of overshoot scenarios on the deep Yedoma carbon is relatively minor compared to stabilization scenarios as well.

This study, like previous ones, uncovers considerable uncertainty in projections of permafrost carbon under global warming. The uncertainty represented by perturbed model parameters for each scenario can be interpreted as model uncertainty. We note that model uncertainty in permafrost carbon releaseloss gradually increases with the peak warming level